

Article

## The Ellipsometry of Anisotropic Manganese Dioxide Films Electrodeposited at Anodic Potentials

\*J.O. Zerbino<sup>a</sup>, #B. A. López de Mishima<sup>b</sup>, \*\*M. López Teijelo<sup>c</sup>, ##A. Maltz<sup>d</sup>,  
and #M. Hernández Úbeda<sup>b</sup>

<sup>a</sup>Instituto de Investigaciones Fisicoquímicas Teóricas y Aplicadas, Suc.4 C.C.16, 1900  
La Plata, Argentina

<sup>b</sup>Instituto de Ciencias Químicas, Fac. de Agronomía y Agroindustrias, Univ. Nac. de  
Santiago del Estero, Avda. Belgrano(s) 1912, 4200 Santiago del Estero, Argentina

<sup>c</sup>Departamento de Fisicoquímica, INFIQC, Facultad de Ciencias Químicas, Univ. Nac.  
de Córdoba, Ag. Postal 4, C.C. 61, 5000 Córdoba, Argentina

<sup>d</sup>Departamento de Matemática, Facultad de Ciencias Exactas, Univ. Nac. de La Plata,  
Calle 50 y 115, 1900 La Plata, Argentina

Received: June 30, 1996; November 28, 1996

A eletrodeposição galvanostática de filmes de dióxido de manganês com espessuras entre 0 e 1000 nm foi investigada por elipsometria *in situ*. Os resultados obtidos podem ser ajustados em termos de uma anisotropia uniaxial do filme para o intervalo completo de espessuras. Os índices ópticos e as espessuras foram calculados. As propriedades anisotrópicas podem ser relacionadas a uma orientação preferencial do depósito.

The galvanostatic electrodeposition of manganese dioxide films in the thickness range from 0 to 1000 nm was investigated by *in situ* ellipsometry. The results obtained can be fit into the whole thickness range in terms of the uniaxial anisotropy of the film. The optical indices and thicknesses were calculated. The anisotropic properties may be related to a preferential orientation of the deposits.

**Keywords:** *ellipsometry, manganese oxide, anisotropy*

### Introduction

The manganese oxides are numerous and many of their structures are poorly known<sup>1</sup>. MnO<sub>2</sub> has been widely studied and many physical and chemical properties such as electrical conductivity, porosity, manganese content, surface area, electrode potential, pore size, and particle shape and size, have been measured and discussed in terms of the dry cell performance<sup>2</sup>. The activity of the manganese oxide layers depends strongly on the deposition conditions<sup>3,4</sup>. The optical characterization of MnO<sub>2</sub> is very valuable for the correlation of *in situ* charge storage capacity and structural changes as a function of the applied potential. How-

ever, ellipsometric studies are limited to a few articles<sup>5,6</sup>. Recently, anodically deposited MnO<sub>2</sub> films were investigated by ellipsometry<sup>7</sup>. Optical results could not be explained as the growth of isotropic or anisotropic layers in the case of thick films and the reported data were interpreted assuming a dependence of the extinction coefficient on the thickness<sup>6,7</sup>.

In the present paper, we report an *in situ* ellipsometric investigation of anodic manganese oxide films grown galvanostatically. The results obtained give evidence of the uniaxial anisotropy of the films, which may be related to a preferential orientation of the deposits.

## Experimental

Manganese oxide films were deposited onto a platinum electrode at a controlled current density from 0.1 M MnSO<sub>4</sub> and 0.17 M H<sub>2</sub>SO<sub>4</sub> solutions. The working platinum electrode (0.95 cm<sup>2</sup> area) was mirror polished with 0.3 and 0.05 μm alumina, rinsed with MilliQ\* water and finally immersed in a conventional optical cell<sup>8</sup>. The wavelength employed was λ = 546.1 nm, with the incident light beam at 70°. Experiments were performed at room temperature under nitrogen bubbling.

The experimental procedures were as follows: the refractive indices of the substrate (n - ik) were obtained at the open circuit potential E<sub>oc</sub> = 0.90 V vs. RHE from the ellipsometric parameters of the recently polished electrode. The resulting values are in good agreement with previously reported data<sup>7,8</sup>. The optical effect of the platinum oxide monolayer can be disregarded<sup>7</sup>.

The Δ and Ψ values during the anodic film growth were measured as follows:

i) every 1 s in a Rudolph Research (vertical type, 2000 FT model) rotating analyzer automatic ellipsometer<sup>7</sup>; ii) every 2 min in a Rudolph Research manual type 437002/200E ellipsometer used in the null mode with the compensator set at 135°<sup>8</sup>.

## Calculation Method

When the optic axis of the uniaxial crystal lies in the plane of incidence, the expressions obtained for ellipsometry are relatively simple. We restricted ourselves to uniaxial films with the optic axis in the direction of stratification, that is, parallel to the z axis<sup>9</sup>. The complete solutions to this particular problem have been previously reported<sup>9-11</sup>.

The experimental data were fit with theoretical models using the gradient techniques<sup>12-14</sup>. The function to be minimized was  $G = \sum (\Delta^{ex} - \Delta^{th})^2 + (\Psi^{ex} - \Psi^{th})^2 + (d - at^b)^2$ , where d is the thickness, t is the time, and a and b are the parameters to be adjusted. The last term was added to fit the closed packed loops corresponding to the high thicknesses. The values of the optical parameters used for calculating these lines were estimated by making initial guesses, then the value of each parameter was varied until a calculated curve was found that better approximated the experimental data in the sense that the root-mean-square deviation of the distance between the point and the curve was reduced. This procedure was repeated using reduced variation of the parameters until the RMS deviation failed to change significantly. If  $G(x_1, \dots, x_m)$  is the differential function to be minimized and  $a = (a_1, \dots, a_m)$  is a point in the m dimensional space, the direction of maximal decrease of G in the position a is given by  $v = -\nabla G(a) = (-\partial G(a)/\partial x_1, \dots, -\partial G(a)/\partial x_m)$ . Different iterative methods are employed to find the

minimum of  $G^{12-14}$  which consist of a succession of approximations  $a_{(0)}, a_{(1)}, a_{(2)}, \dots$  in the m dimensional space converging on the solution  $b = (b_1, \dots, b_m)$  which is attained within the degree of accuracy required.

When the convergence of the approximations is fulfilled, then: a)  $G_{(a_{(0)})} > G_{(a_{(1)})} > G_{(a_{(2)})}, \dots$ ; b)  $\partial G_{(a_{(n)})}/\partial x_i$  will tend to 0 as n increases; and c) the distances  $\|a_{(n)} - a_{(n+1)}\|$  will tend to 0 for increasing n.

## The Anisotropic Model

The effect of uniaxial anisotropy is to displace the successive loops parallel to the axis by an amount that depends on the magnitude of the anisotropy and in a direction that depends on whether the film is uniaxial positive or uniaxial negative<sup>15</sup>. For an experimental configuration in which the quarter-wave plate is placed at 45 degrees between the polarizer and the sample, a uniaxial positive film ( $n_z > n_x = n_y$ ) will cause successive loops to be displaced towards lower values, whereas a uniaxial negative film ( $n_z < n_x = n_y$ ) will cause a displacement towards higher values.

For non-absorbing materials, and assuming an assembly of parallel cylindrical rods of index  $n_1$ , immersed in a medium of index  $n_2$ , the structure will be uniaxially positive<sup>15-16</sup>:

$$n_z^2 - n_x^2 = \frac{f_1 f_2 (n_1^2 - n_2^2)^2}{[(1 + f_1) n_2^2 + f_2 n_1^2]} \quad (1)$$

where  $f_1$  and  $f_2$  are the fractions of the total volume occupied by the rods and the medium and  $f_1 \ll 1$ .  $n_z^2 - n_x^2$  will always be positive for  $n_1^2 > n_2^2$  or  $n_1^2 < n_2^2$ .

Analogously, for an assembly of particles that have the form of thin parallel plates, Eq. 1 may be written as:

$$n_z^2 - n_x^2 = \frac{f_1 f_2 (n_1^2 - n_2^2)^2}{f_1 n_2^2 + f_2 n_1^2} \quad (2)$$

This implies that the assembly always behaves like a negative uniaxial crystal.

## Results and Discussion

The Δ vs. Ψ plot obtained by applying an anodic current density  $i = 100 \mu\text{A cm}^{-2}$  for a total time of 45 min is shown in Fig. 1. Experimental measurements were obtained with the automatic ellipsometer for negative values of ellipticity. In this case, the errors in the azimuth were larger when the ellipticity approached 45 degrees; therefore the indetermination in the Δ and Ψ values also increases under these conditions<sup>17</sup>. In the same figure the theoretical fitted curve is plotted, obtained according to the calculation method described above.

The theoretical curve (assuming optical indices independent of the thickness) fits the experimental data in the whole range of thicknesses reproducing the various loops. Assuming a uniaxial anisotropic film with the optical axis coinciding with the axis normal to the surface results in the optical indices  $n_p = 1.788$ ,  $n_s = 1.756$ ,  $k_p = 0.0187$ ,  $k_s = 0.2260$ . The corresponding time vs. thickness plot shows a linear dependence (Fig. 2).

A similar galvanostatic experiment for  $i = 44 \mu\text{A cm}^{-2}$  for a total time of 110 min, obtained with the manual ellipsometer, is shown in Fig. 3. The fitting was performed taking different sets of data corresponding to increasing ranges of thickness. Fig. 3a shows the fitted curve obtained for  $10 < d < 130 \text{ nm}$ , whereas in Fig. 3b the curve for

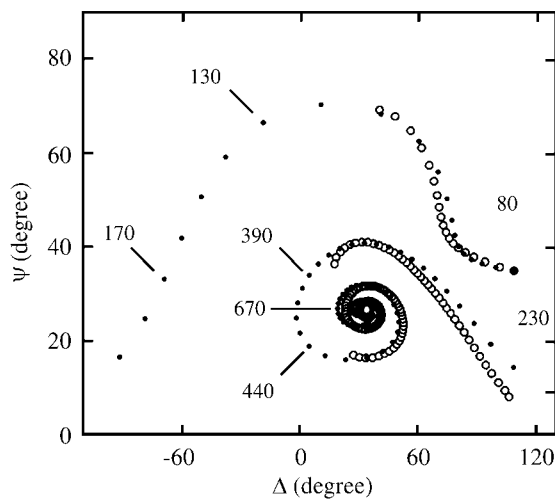


**Figure 1.** The evolution of the ellipsometric parameters  $\Delta$  and  $\Psi$  using the automatic ellipsometer.  $i = 100 \mu\text{A cm}^{-2}$ . The figures indicate the thicknesses  $d$  in nm.

(•) Theoretical curve for thickness increments of 10 nm. (o) Experimental points.

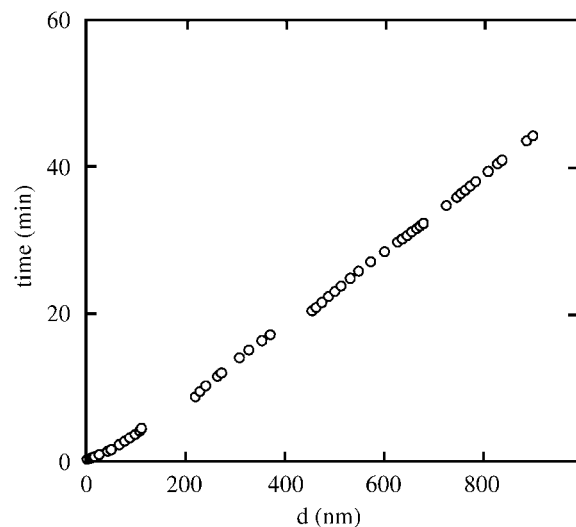


**Figure 2.** The time vs. thickness plot corresponding to the experiment of Fig. 1.

$200 < d < 730 \text{ nm}$  range is included. The values of optical indices corresponding to the different ranges show a slight dependence on  $d$  (Fig. 4). Nevertheless, the calculated thicknesses are almost independent of the chosen range of thickness (upper part of Fig. 4), indicating that the calculated thicknesses are not strongly dependent on the variation in the optical indices obtained.

For isotropic materials, the dependence of  $n$  and  $k$  on the volume fraction of the composite,  $f_i$  can be tested with effective medium theories<sup>8</sup>. In the case of birefringent layers, the number of fitted parameters increases and the relationship between composition or density of the film and optical indices is uncertain. Therefore, only the average optical indices, independent of thickness, were considered significant.

The refractive indices and absorption coefficients calculated, assuming optical properties independent of thick-

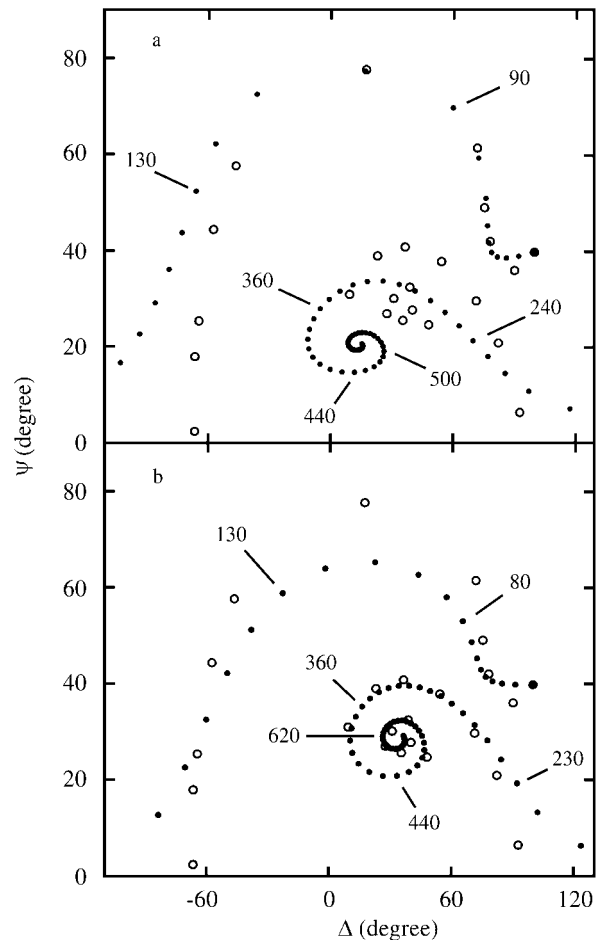


**Figure 3.** The  $\Delta$  and  $\Psi$  plot obtained using the manual ellipsometer.  $i = 44 \mu\text{A cm}^{-2}$ .

(•) Theoretical curve. (o) Experimental measurements.

A) Theoretical fitting in the  $10 < d < 130 \text{ nm}$  range; B) in the  $200 < d < 730 \text{ nm}$  range.

The figures indicate the thickness  $d$  in nm.

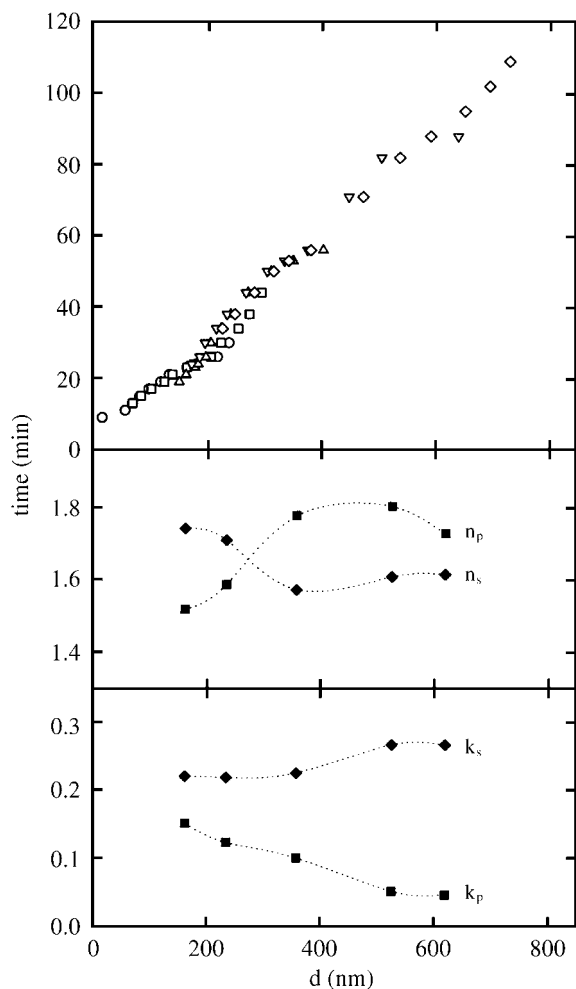


**Figure 4.** Refractive indices  $n_s$ , and  $n_p$ , and the absorption coefficients  $k_s$  and  $k_p$ , and the deposition time as a function of thickness for the experiment of Fig. 3.

ness, or adsorption of oriented molecules<sup>8,21-33</sup>. Pores or needles could also cause a structural directional anisotropy.

The optical anisotropy shown by  $MnO_2$  films may be related to the deposit morphology. Electrolytic manganese dioxide is usually described as a  $\gamma$  or  $\epsilon$ - $MnO_2$  structure<sup>34</sup>. The  $\gamma$  material was reported as microporous or consisting of needle-shaped particles<sup>35</sup>. The  $\gamma$ - $MnO_2$  made up of flat needles of  $40,000 \times 2,000 \times 500 \text{ \AA}$  have been obtained by treating  $Mn_3O_4$  with diluted nitric acid<sup>36</sup>. The morphology of  $MnO_2$  obtained by anodic oxidation of  $Mn^{2+}$  depends on both composition and current density<sup>37-38</sup>. Polycrystalline  $MnO_2$  with a random distribution of the lattice orientations is obtained in hot sulfuric acid containing  $MnSO_4$ , whereas acidic solutions of chloride, nitrate, or perchlorate, exhibit a fibrous structure, the fibers being parallel to the direction of growth. However, it has been demonstrated by X-ray diffraction that it is possible to produce a fibrous manganese dioxide from an acidified sulfate bath<sup>39,40</sup>.

The optical indices obtained for the anisotropic  $MnO_2$  (Fig. 4) indicate that the  $n_p$  and  $n_s$  values are comparable, while  $k_s$  is certainly higher than  $k_p$ . This behavior may be related to a preferential orientation of micro fibers in the deposit. The fitting procedure assuming constant indices independent of thickness, indicates that the structure of the deposits remains relatively constant during growth.

Further work on the dependence of the anisotropic optical indices for different deposition conditions will provide more useful information to elucidate this complex deposition mechanism<sup>41</sup>.

### Acknowledgments

This research was supported by the Consejo Nacional de Investigaciones Científicas (CONICET), the Comisión de Investigaciones Científicas de la Provincia de Buenos Aires (CIC), and the Fundación Antorchas. B.A. López de Mishima and M. López Teijelo are research members of CONICET and J.O. Zerbino is a researcher with CIC.

### References

1. Turner, S.; Buseck, P.R. *Science* **1979**, *203*, 456. Idem **1981**, *212*, 1024.
2. Fernández, J.B.; Desai, B.; Kamat Dalal, V.N. *Electrochim. Acta* **1983**, *28*, 309.
3. Welsh, J.Y. *Electrochem. Technol.* **1967**, *5*, 504.
4. Brenet, J.P. *Electrochim. Acta* **1959**, *1*, 231.
5. Spricis, A.A.; Slaidins, G.J.; Abele, J.J.; Dzelme, J.R. *Elektrokhimiya* **1982**, *18*, 339.
6. Ord, J.L.; Huang, Z.Q. *J. Electrochem. Soc.* **1985**, *132*, 1183.
7. Hernández Ubeda, M.; López de Mishima, B.A.; Zerbino, J.O.; López Teijelo, M. *Electrochim. Acta* in press.
8. Zerbino, J.O.; Perdriel, C.; Arvia, A.J. *Thin Solid Films* **1993**, *232*, 63.
9. den Engelsen, D. *J. Opt. Soc. Am.* **1971**, *61*, 1460.
10. Cornish, W.D.; Young, L. *Proc. R. Soc. Lond. A.* **1973**, *335*, 39.
11. Dignam, M.J.; Moskovits, M.; Stobie, R.W. *Trans. Faraday Soc.* **1971**, *67*, 3306.
12. Beltrami, E.J. In *An algorithmic approach to nonlinear analysis and optimization*; Bellman, R.; Ed.; Academic Press, 1970, pp. 27-35.
13. Polak, E. In *Computational Methods in Optimization*; Bellman, R.; Ed.; Academic Press, 1971, pp. 28-30.
14. Dahlquist, G.; Bjorck, A. In *Numerical Methods*; Prentice-Hall, 1974, pp. 441-43.
15. Clayton, J.C.; De Smet, D.J. *J. Electrochem. Soc.* **1976**, *123*, 1886.
16. Born, M.; Wolf, E. In *Principles of Optics*; Pergamon Press, 1975, pp. 705-08.

17. Rudolph Research, *2000 FT Users Manual. Revision 6.0*, Flanders, N.J., USA.
18. Lenham, A.P. *Proc. Phys. Soc.* **1963**, 82, 933.
19. Lenham, A.P.; Treherne, D.M.; Metcalfe, R.J. *J. Opt. Soc. Am.* **1965**, 55, 1072.
20. Meyer, F.; de Kluizernaar, E.E.; den Engelsen, D. *J. Opt. Soc. Am.* **1973**, 63, 529.
21. Azzam, R.M.A.; Bashara, N.M. *J. Opt. Soc. Am.* **1972**, 62, 1375.
22. Chan, E.C.; Marton, J.P. *J. Appl. Physics* **1974**, 45, 5004.
23. Yamaguchi, T.; Yoshida, S.; Kinbara, A. *J. Op. Soc. Am.* **1972**, 62, 634.
24. Ord, J.L.; De Smet, D.J. *J. Electrochem. Soc.* **1992**, 139, 359.
25. Ord, J.L.; De Smet, D.J. *J. Electrochem. Soc.* **1992**, 139, 728.
26. Jacobsen, T.; Kerker, M. *J. Opt. Soc. Am.* **1967**, 57, 751.
27. Matthews, C.G.; Ord, J.L.; Wang, W.P. *J. Electrochem. Soc.* **1983**, 130, 285.
28. Ord, J.L.; Clayton, J.C.; Brudzewski, K. *J. Electrochem. Soc.* **1978**, 125, 908.
29. Ord, J.L.; Wang, W.P. *J. Electrochem. Soc.* **1983**, 130, 1809.
30. Bean, C.P. In *Structures and properties of thin films*; Proc. Int. Conf. Bolton Landing, Sep. 9-11, 1959, Neugebauer, D.C.A., Ed; John Wiley & Sons, Inc.
31. Venturini, E.L.; Spencer, E.G.; Lenzo, P.V.; Ballman, A.A. *J. Appl. Phys.* **1968**, 39, 343.
32. Lenzo, P.V.; Spencer, E.G.; Ballman, A.A. *Appl. Phys. Lett.* **1967**, 11, 23.
33. den Engelsen, D. *J. Phys. Chem.* **1972**, 76, 3390.
34. Ruetschi, P. *J. Electrochem. Soc.* **1988**, 135, 2657.
35. Ghosh, S.; Brenet, J.P. *Electrochim. Acta* **1962**, 7, 449.
36. Giovanoli, R.; Maurer, R.; Feitknecht, W. *Helv. Chim. Acta* **1967**, 50, 1072.
37. Matsuki, K.; Endo, T.; Kamada, H. *Electrochim. Acta* **1984**, 29, 983.
38. Amano, Y. *U. S. Patent*, **1970**, 3, 535, 217; Amano, Y.; Kumano, H.; Nishino, A.; Noguchi, Y. *Japanese Patent* 1972, 47, 2419.
39. Preisler, E. *J. Appl. Electrochem.* **1976**, 6, 301.
40. Preisler, E. *Electrochim. Acta* **1981**, 26, 1389.
41. Zerbino, J.O.; López de Mishima, B.A.; Hernández Úbeda, M.; López Teijelo, M. In preparation.